Supplement to: Assessing CMIP6 uncertainties at global warming levels

Guillaume Evin[1*], Aurélien Ribes[2] and Lola Corre[3]

[1*]Univ. Grenoble Alpes, INRAE, CNRS, IRD, Grenoble INP, IGE, Grenoble, 38000, France.
[2]Centre National de Recherches Météorologiques, Université de Toulouse, Météo-France, CNRS, Toulouse, France.
[3]Centre National de Recherches Météorologiques, Université de Toulouse, Météo-France, CNRS, Toulouse, France.

*Corresponding author(s). E-mail(s): guillaume.evin@inrae.fr;
Contributing authors: aurelien.ribes@meteo.fr; lola.corre@meteo.fr;

S1 Characteristics of the scenarios

Table S1 Characteristics of the scenarios of the CMIP6 climate projection ensemble.

GCM	SSP scenario	List of members
ACCESS-CM2	ssp245	r1i1p1f1 / r2i1p1f1 / r3i1p1f1 / r4i1p1f1 / r5i1p1f1
ACCESS-CM2	ssp370	r1i1p1f1 / r2i1p1f1 / r3i1p1f1 / r4i1p1f1 / r5i1p1f1
ACCESS-CM2	ssp585	r10i1p1f1 / r1i1p1f1 / r2i1p1f1 / r3i1p1f1 / r4i1p1f1 / r5i1p1f1 / r6i1p1f1 / r7i1p1f1 / r8i1p1f1 / r9i1p1f1
CanESM5	ssp245	r10i1p1f1 / r1i1p1f1 / r2i1p1f1 / r3i1p1f1 / r4i1p1f1 / r5i1p1f1 / r6i1p1f1 / r7i1p1f1 / r8i1p1f1 / r9i1p1f1
CanESM5	ssp370	r10i1p1f1 / r1i1p1f1 / r2i1p1f1 / r3i1p1f1 / r4i1p1f1 / r5i1p1f1 / r6i1p1f1 / r7i1p1f1 / r8i1p1f1 / r9i1p1f1
CanESM5	ssp585	r10i1p1f1 / r1i1p1f1 / r2i1p1f1 / r3i1p1f1 / r4i1p1f1 / r5i1p1f1 / r6i1p1f1 / r7i1p1f1 / r8i1p1f1 / r9i1p1f1
CNRM-ESM2-1	ssp245	r10i1p1f2 / r1i1p1f2 / r2i1p1f2 / r3i1p1f2 / r4i1p1f2 / r5i1p1f2 / r6i1p1f2 / r7i1p1f2 / r8i1p1f2 / r9i1p1f2
CNRM-ESM2-1	ssp370	r1i1p1f2 / r2i1p1f2 / r3i1p1f2 / r4i1p1f2 / r5i1p1f2
CNRM-ESM2-1	ssp585	r1i1p1f2 / r2i1p1f2 / r3i1p1f2 / r4i1p1f2 / r5i1p1f2
IPSL-CM6A-LR	ssp245	r10i1p1f1 / r1i1p1f1 / r2i1p1f1 / r3i1p1f1 / r4i1p1f1 / r5i1p1f1 / r6i1p1f1
IPSL-CM6A-LR	ssp370	r10i1p1f1 / r1i1p1f1 / r2i1p1f1 / r3i1p1f1 / r4i1p1f1 / r5i1p1f1 / r6i1p1f1 / r7i1p1f1 / r8i1p1f1 / r9i1p1f1
IPSL-CM6A-LR	ssp585	r1i1p1f1 / r2i1p1f1 / r3i1p1f1 / r4i1p1f1 / r6i1p1f1
MIROC6	ssp245	r10i1p1f1 / r1i1p1f1 / r2i1p1f1 / r3i1p1f1 / r4i1p1f1 / r5i1p1f1 / r6i1p1f1 / r7i1p1f1 / r8i1p1f1 / r9i1p1f1
MIROC6	ssp370	r10i1p1f1 / r1i1p1f1 / r2i1p1f1 / r3i1p1f1 / r4i1p1f1 / r5i1p1f1 / r6i1p1f1 / r7i1p1f1 / r8i1p1f1 / r9i1p1f1
MIROC6	ssp585	r10i1p1f1 / r1i1p1f1 / r2i1p1f1 / r3i1p1f1 / r4i1p1f1 / r5i1p1f1 / r6i1p1f1 / r7i1p1f1 / r8i1p1f1 / r9i1p1f1
MPI-ESM1-2-LR	ssp245	r10i1p1f1 / r1i1p1f1 / r2i1p1f1 / r3i1p1f1 / r4i1p1f1 / r5i1p1f1 / r6i1p1f1 / r7i1p1f1 / r8i1p1f1 / r9i1p1f1
MPI-ESM1-2-LR	ssp370	r10i1p1f1 / r1i1p1f1 / r2i1p1f1 / r3i1p1f1 / r4i1p1f1 / r5i1p1f1 / r6i1p1f1 / r7i1p1f1 / r8i1p1f1 / r9i1p1f1
MPI-ESM1-2-LR	ssp585	r10i1p1f1 / r1i1p1f1 / r2i1p1f1 / r3i1p1f1 / r4i1p1f1 / r5i1p1f1 / r6i1p1f1 / r7i1p1f1 / r8i1p1f1 / r9i1p1f1
UKESM1-0-LL	ssp245	r10i1p1f2 / r1i1p1f2 / r2i1p1f2 / r3i1p1f2 / r4i1p1f2 / r5i1p1f2 / r6i1p1f2 / r7i1p1f2 / r8i1p1f2 / r9i1p1f2
UKESM1-0-LL	ssp370	r10i1p1f2 / r1i1p1f2 / r2i1p1f2 / r3i1p1f2 / r4i1p1f2 / r5i1p1f2 / r6i1p1f2 / r7i1p1f2 / r8i1p1f2 / r9i1p1f2
UKESM1-0-LL	ssp585	r1i1p1f2 / r2i1p1f2 / r3i1p1f2 / r4i1p1f2 / r8i1p1f2

S2 Illustration of the QUALYPSO approach

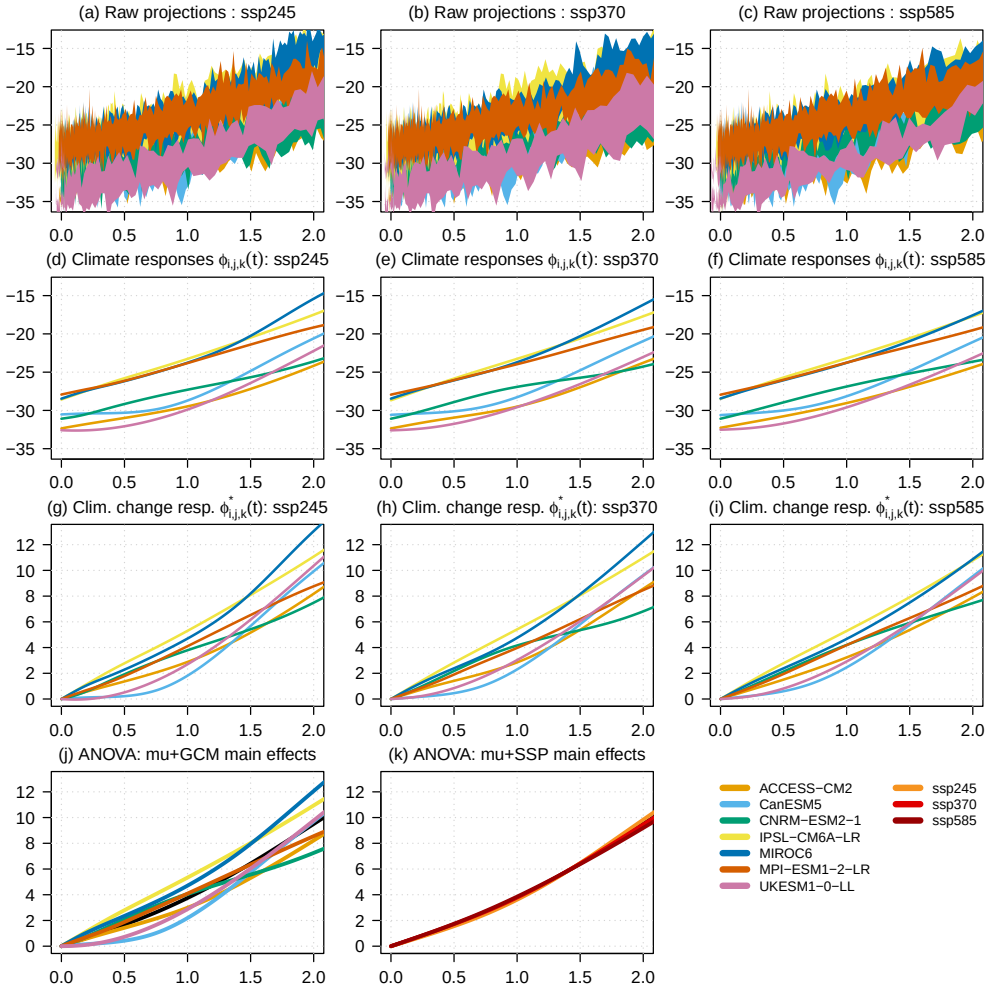

Fig. S1 Illustration of the QUALYPSO approach for mean winter temperature in the AR6 reference region ARO, in [°C], when it is applied as a function of the warming level. Each column corresponds to a scenario SSP. (a-c) "Raw" climate projections: intervals covered by the different members available for each scenario/GCM combination (one color by GCM). (d-f) Climate responses $\phi_{g,s}(GWL)$. (g-i) Climate change responses $\phi^{\star}_{g,s}(GWL)$. (j) Illustration of the ANOVA for GCM main effects $(\mu(GWL) + \alpha_g(GWL))$. The black line shows the mean climate change response μ. The dispersion (variance) between the main GCM effects provides an estimate of the GCM uncertainty. (k) Illustration of the ANOVA for SSP main effects $(\mu(GWL) + \beta_s(GWL))$.

S3 Climate responses as a function of warming level

Figs. S2-S9 present the multi-member projections for each GCM and different reference regions, and the corresponding climate responses obtained for the different SSP scenarios.

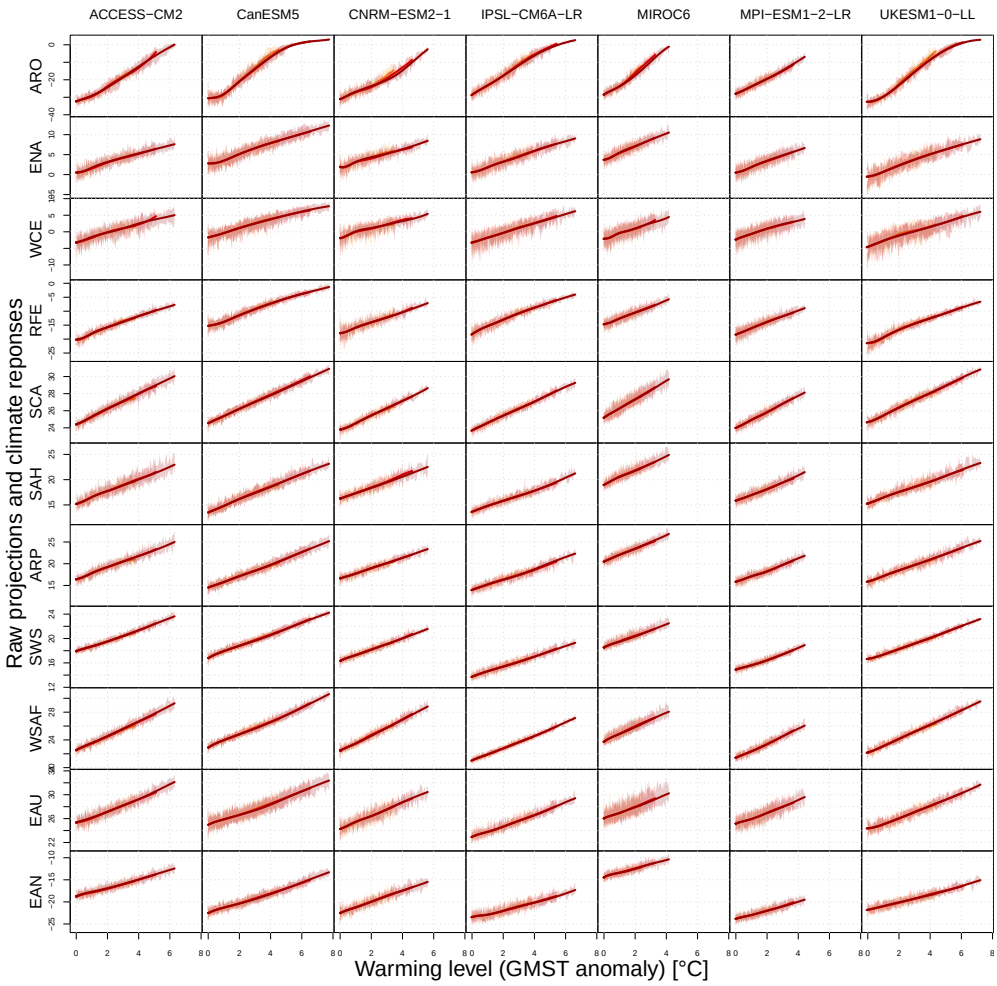

Fig. S2 Raw projections of DJF temperature (transparent band) and corresponding climate responses (plain line). Each column corresponds to a GCM and each line to an illustrative IPCC WGI reference region. The different colors refer to the three different SSPs (see legend of Fig. S1).

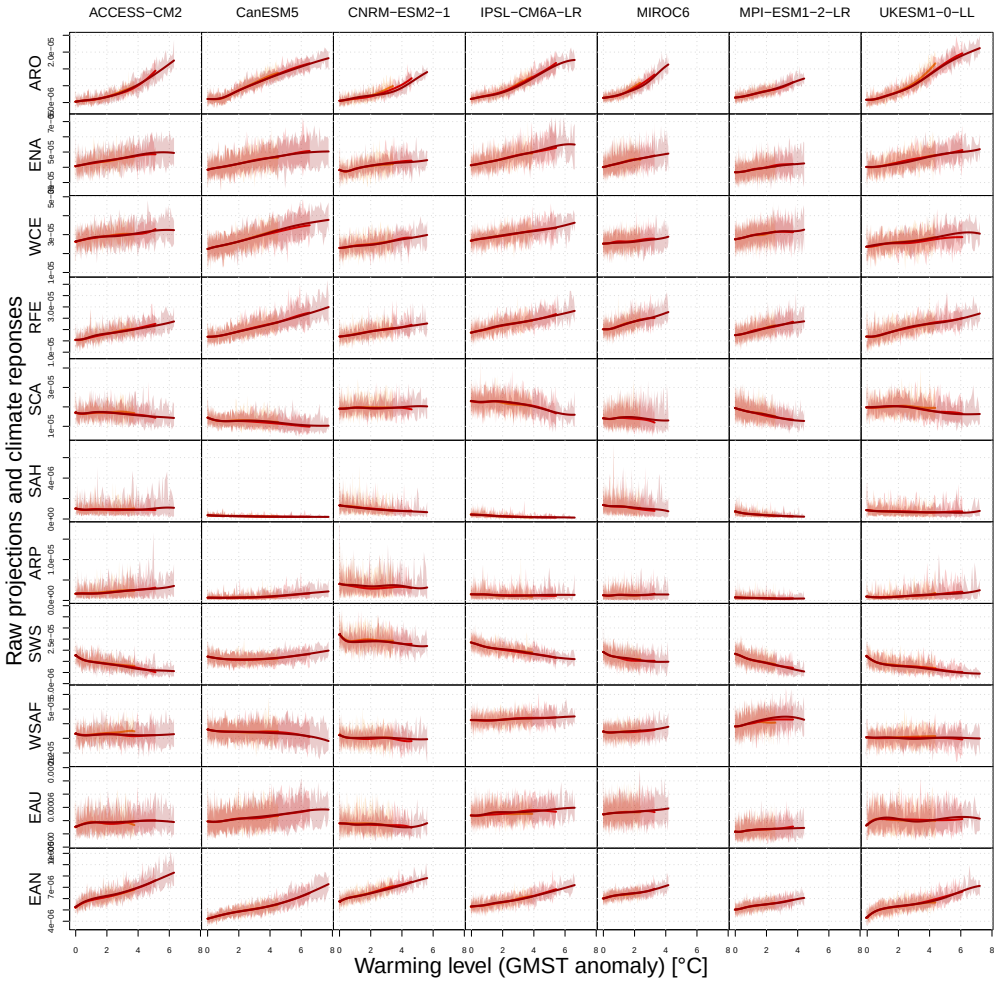

Fig. S3 Raw projections of DJF precipitation (transparent band) and corresponding climate responses (plain line). Each column corresponds to a GCM and each line to an illustrative IPCC WGI reference region. The different colors refer to the three different SSPs (see legend of Fig. S1).

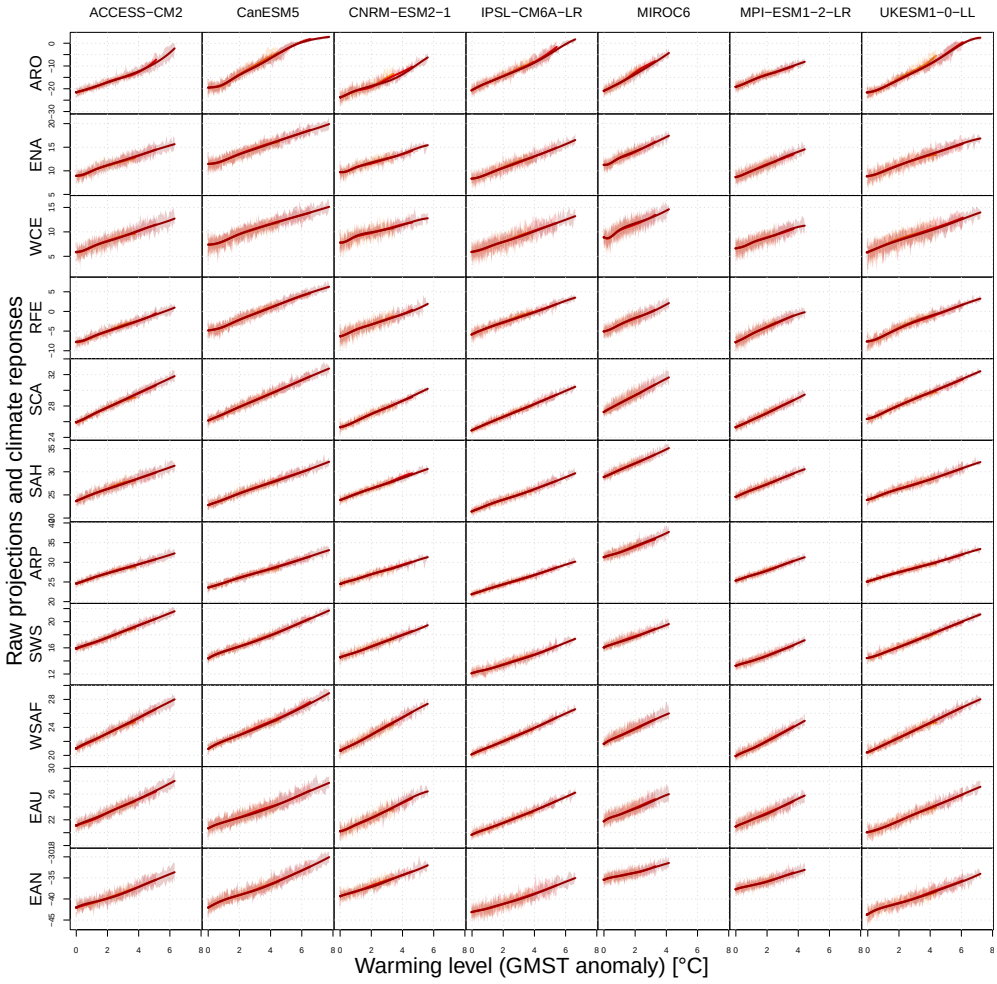

Fig. S4 Raw projections of MAM temperature (transparent band) and corresponding climate responses (plain line). Each column corresponds to a GCM and each line to an illustrative IPCC WGI reference region. The different colors refer to the three different SSPs (see legend of Fig. S1).

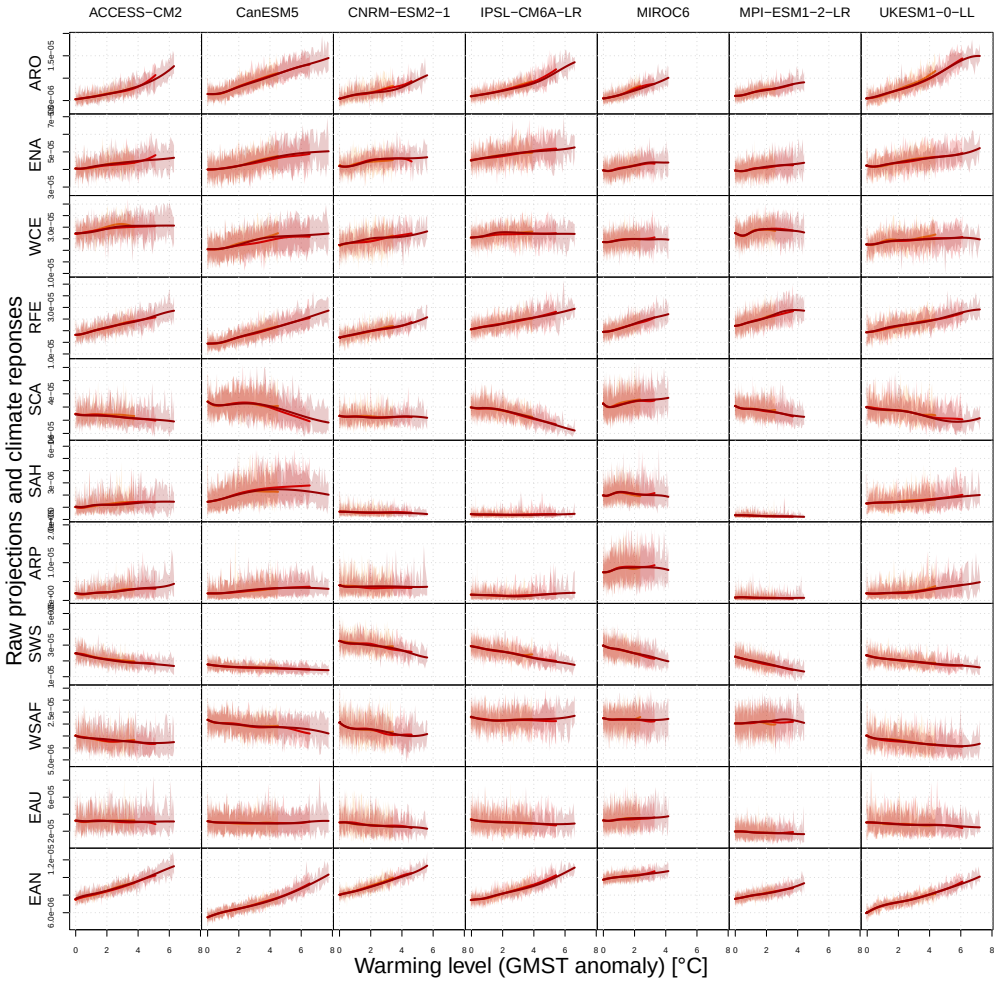

Fig. S5 Raw projections of MAM precipitation (transparent band) and corresponding climate responses (plain line). Each column corresponds to a GCM and each line to an illustrative IPCC WGI reference region. The different colors refer to the three different SSPs (see legend of Fig. S1).

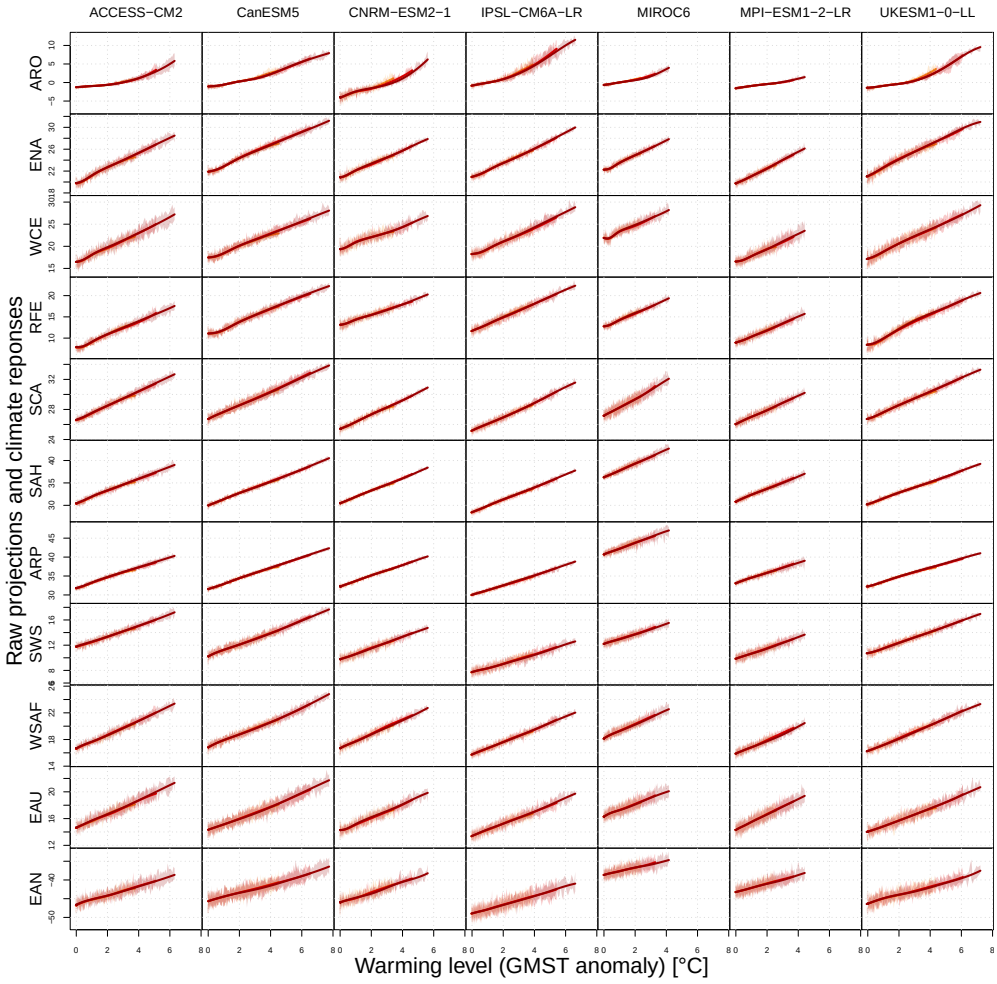

Fig. S6 Raw projections of JJA temperature (transparent band) and corresponding climate responses (plain line). Each column corresponds to a GCM and each line to an illustrative IPCC WGI reference region. The different colors refer to the three different SSPs (see legend of Fig. S1).

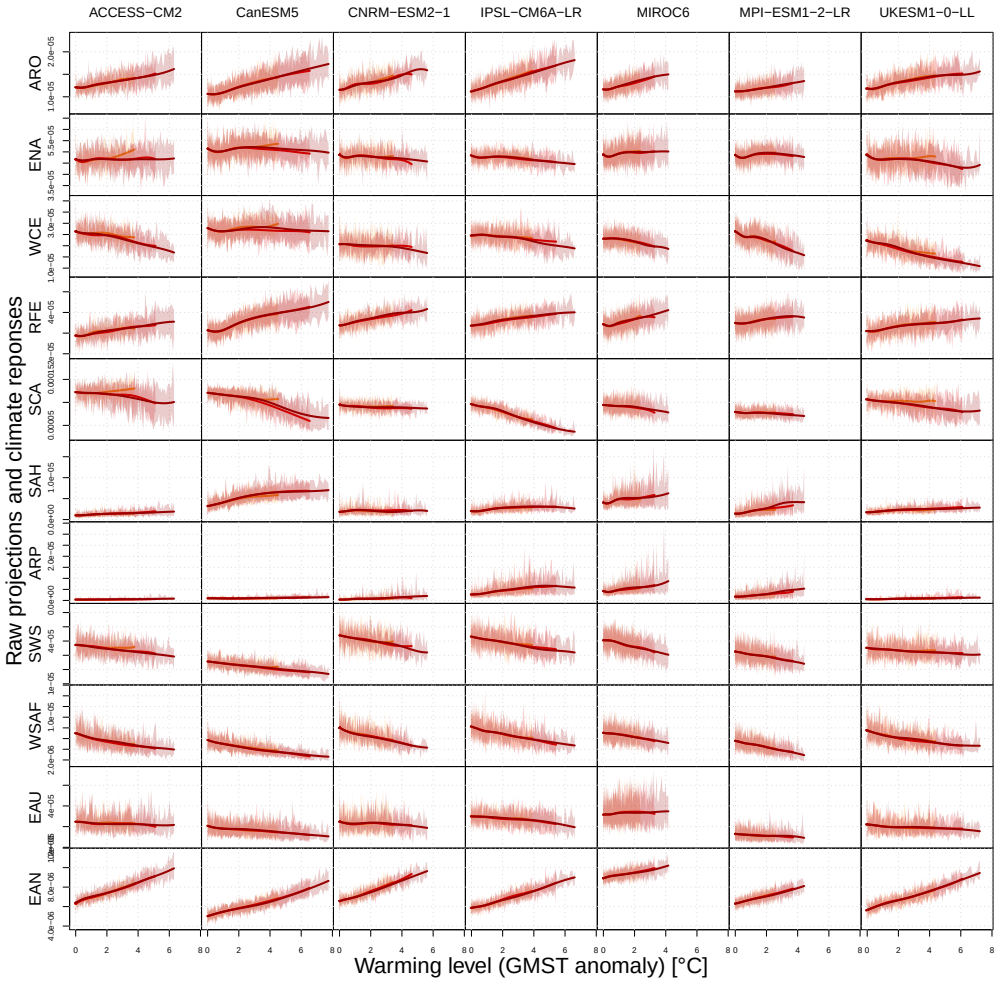

Fig. S7 Raw projections of JJA precipitation (transparent band) and corresponding climate responses (plain line). Each column corresponds to a GCM and each line to an illustrative IPCC WGI reference region. The different colors refer to the three different SSPs (see legend of Fig. S1).

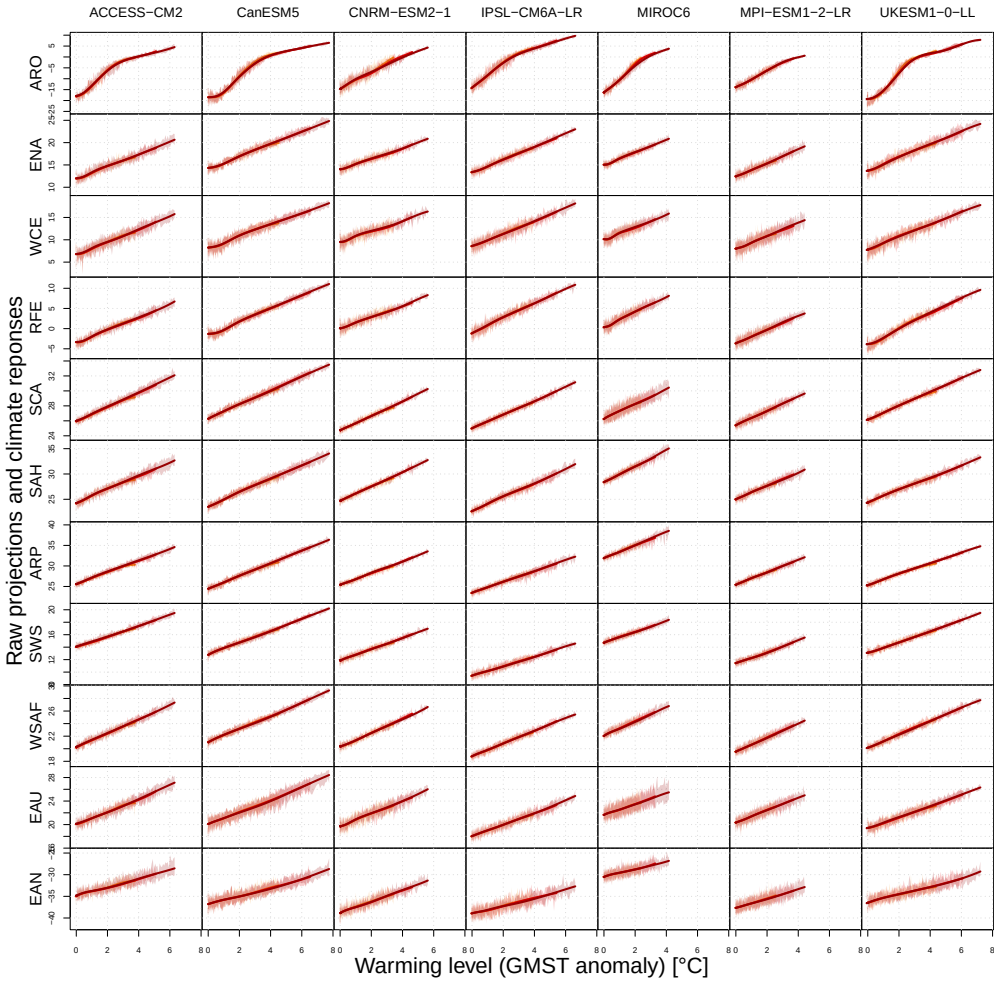

Fig. S8 Raw projections of SON temperature (transparent band) and corresponding climate responses (plain line). Each column corresponds to a GCM and each line to an illustrative IPCC WGI reference region. The different colors refer to the three different SSPs (see legend of Fig. S1).

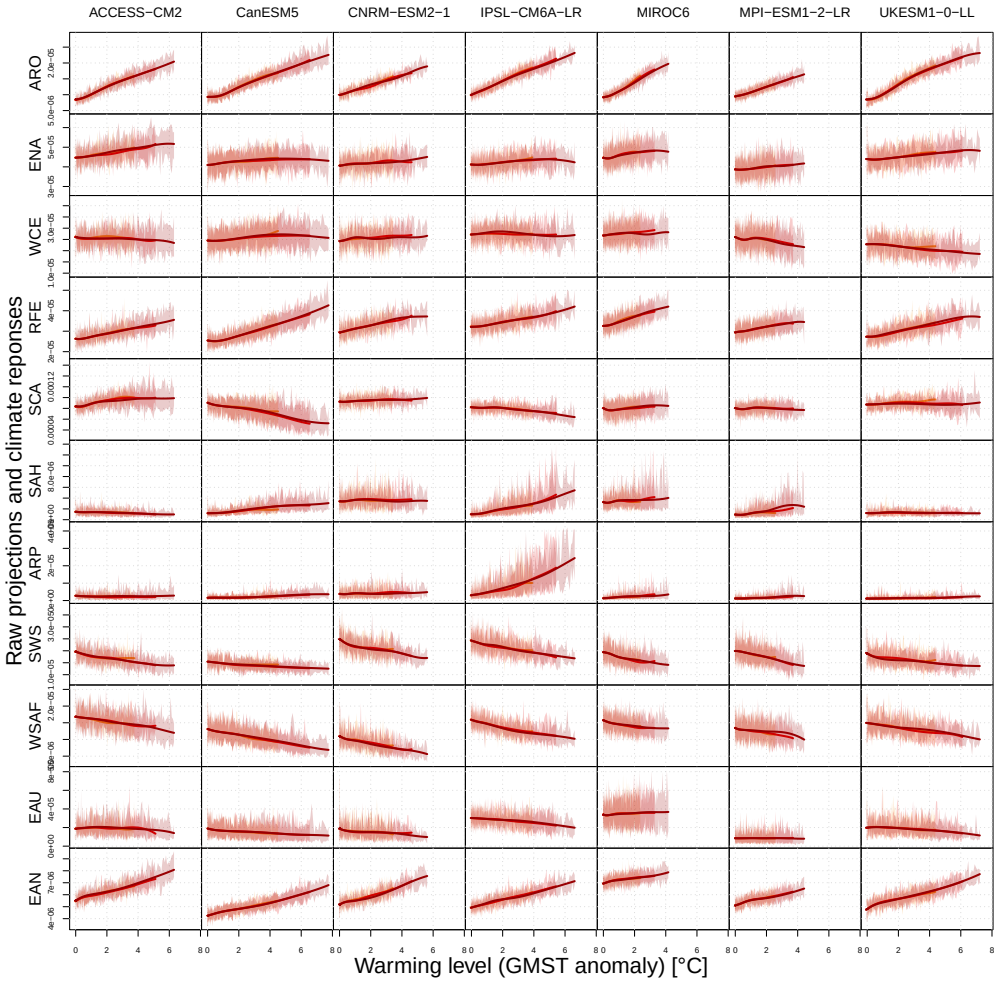

Fig. S9 Raw projections of SON precipitation (transparent band) and corresponding climate responses (plain line). Each column corresponds to a GCM and each line to an illustrative IPCC WGI reference region. The different colors refer to the three different SSPs (see legend of Fig. S1).

S4 Supplementary results in winter (DJF) and summer (JJA)

S4.1 Spatial variability of the total uncertainty at a 1° X 1° resolution

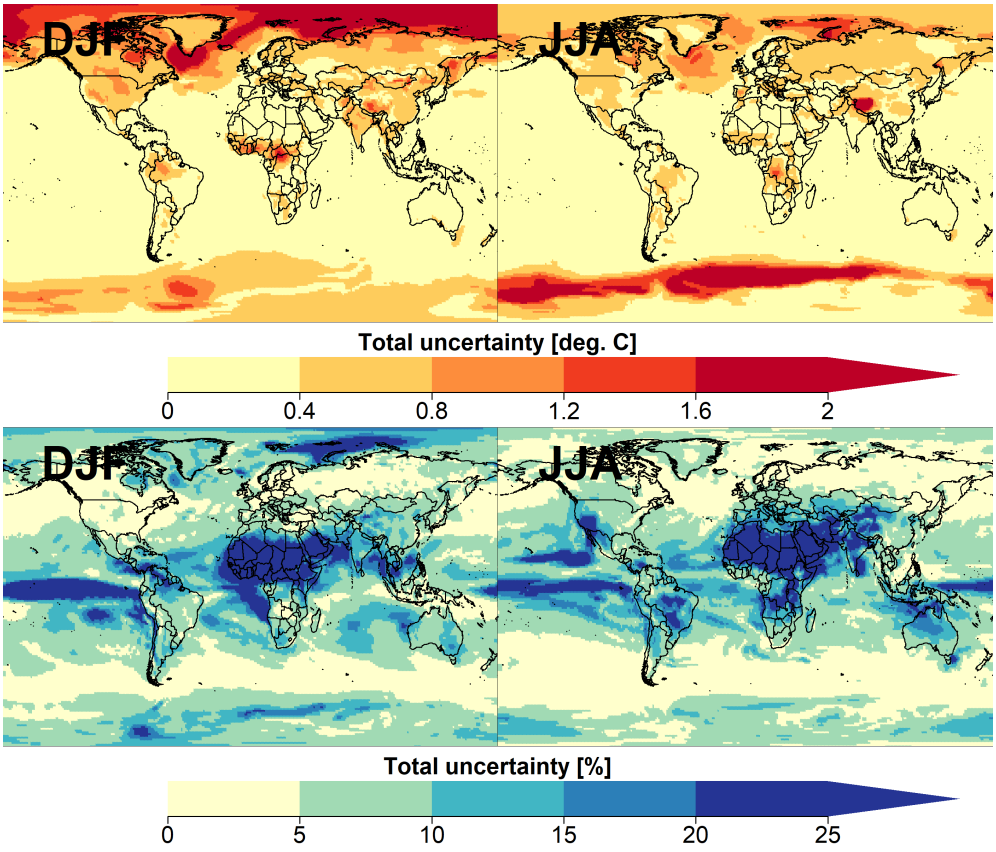

Fig. S10 Total uncertainty $TU(2)$ (square root of the total variance) at a 1° × 1° resolution, for absolute changes of mean temperature (tas) and relative changes of total precipitation (pr) in winter (DJF) and summer (JJA) at a warming level of +2°C compared with the pre-industrial period (1850–1900).

S4.2 Climate change responses at a warming level of +2°C

Figure S11 shows the climate change responses of mean seasonal temperature and precipitation for a +2°C warming level compared with the pre-industrial period (1850–1900), for each GCM and forcing scenario.

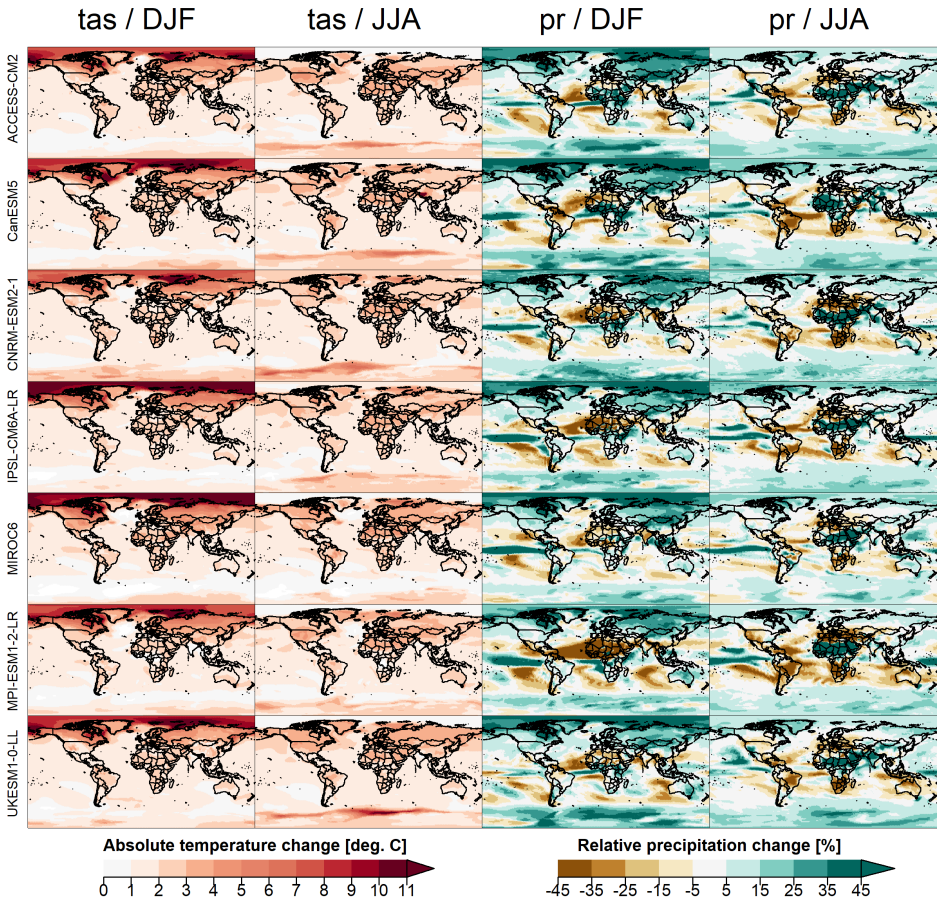

Fig. S11 Climate change responses in winter (DJF) and summer (JJA) at a warming level of +2°C compared with the pre-industrial period (1850–1900), for the SSP585. Each row corresponds to a GCM and each column to a different variable/season.

S4.3 Contribution of each GCM to the GCM uncertainty

Figure S12 provides maps showing the areas where a GCM has a contribution greater than 50% to the GCM uncertainty, in winter (DJF) and summer (JJA).

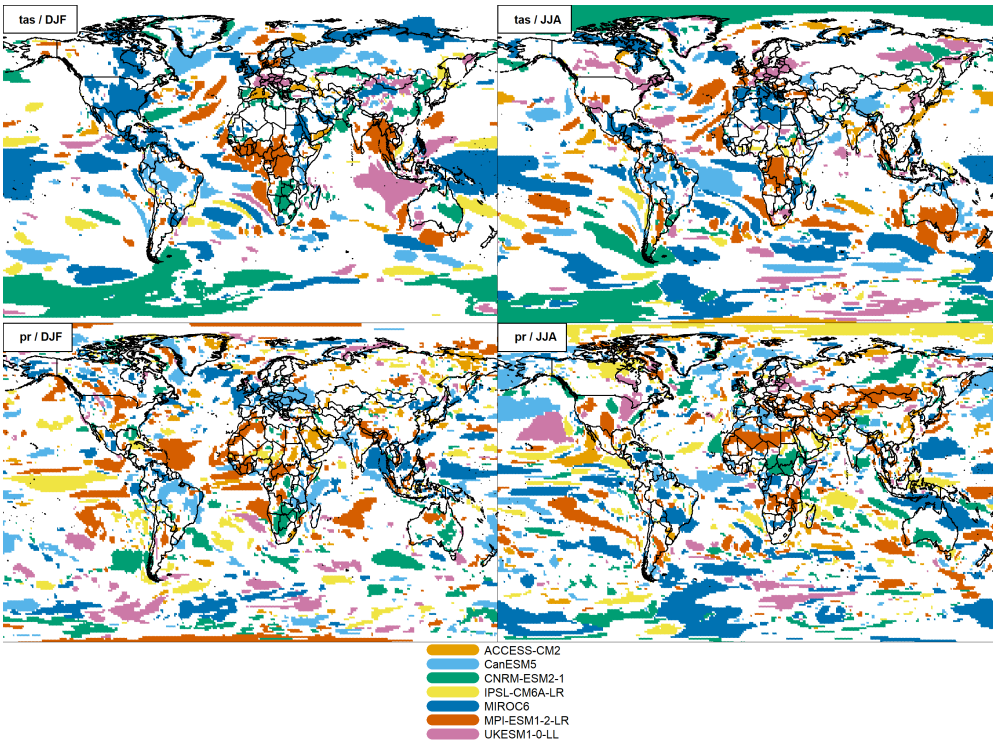

Fig. S12 GCM with a contribution greater than 50% to the GCM uncertainty at a 1° × 1° resolution for absolute temperature (top plots) and relative precipitation changes (bottom plots), in winter (DJF) and summer (JJA) at a warming level of +2°C compared with the pre-industrial period (1850–1900).

S5 Supplementary results in spring (MAM) and autumn (SON)

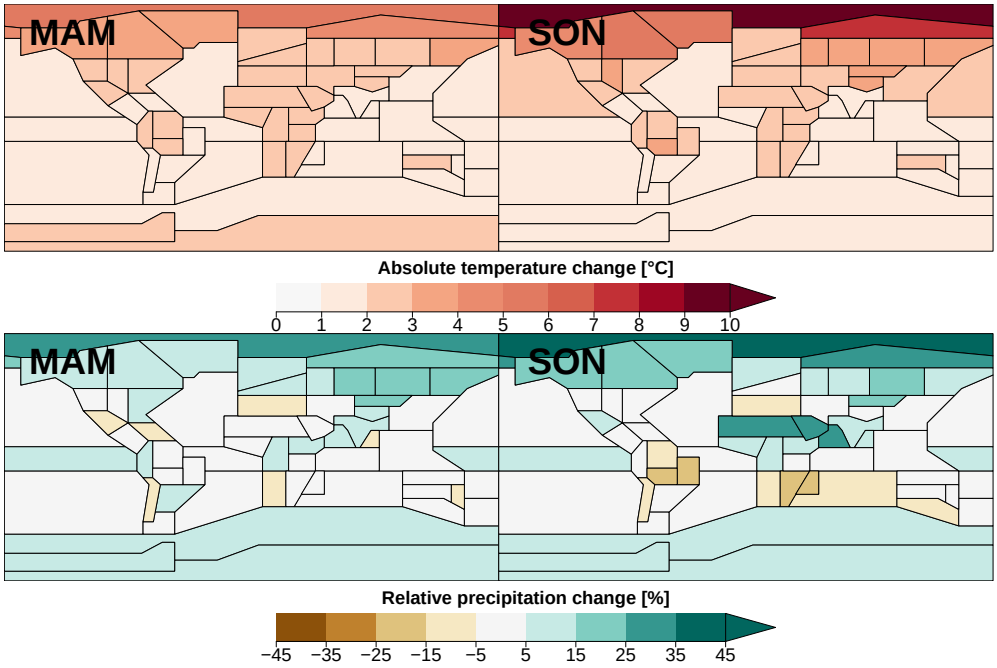

Fig. S13 Mean climate change response in spring (MAM) and autumn (SON) at a warming level of +2°C compared with the pre-industrial period (1850–1900), for absolute changes of temperature (top plots) and relative changes of precipitation (bottom plots).

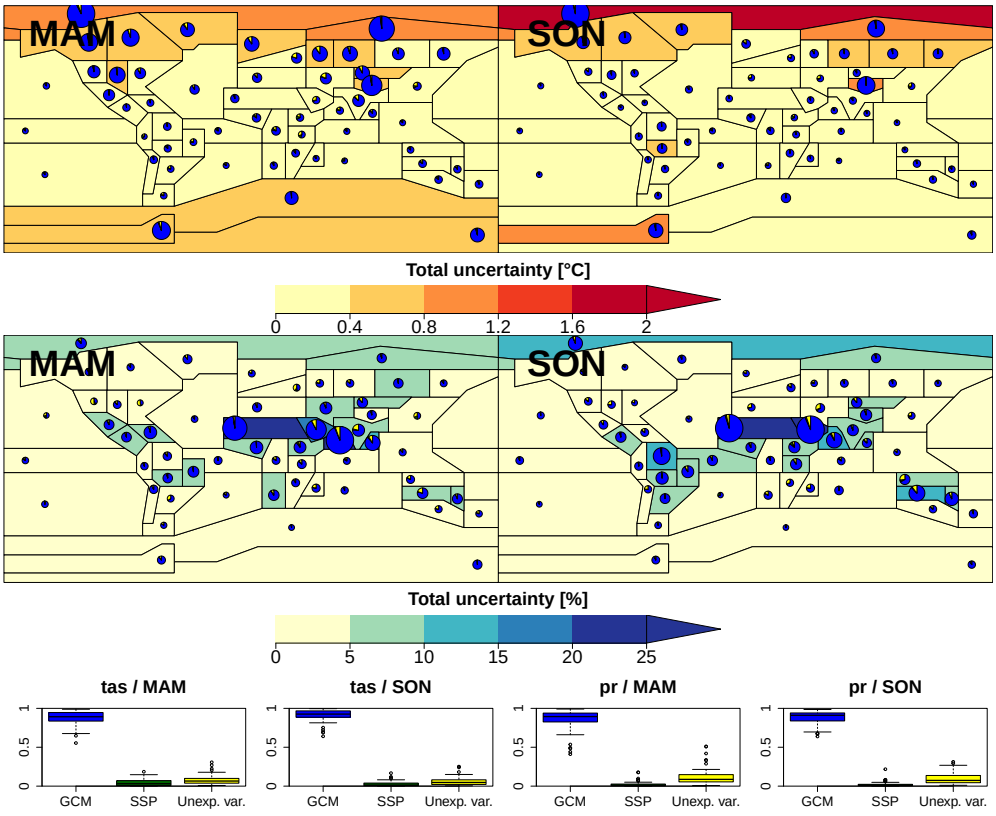

Fig. S14 Total uncertainty $TU(2)$ (square root of the total variance) for absolute changes of mean temperature (tas) and relative changes of total precipitation (pr) in spring (MAM) and autumn (SON) at a warming level of +2°C compared with the pre-industrial period (1850–1900). For each reference region, the pie chart provides the contributions of the different components to the total uncertainty (GCM in blue, scenario SSP in green, and unexplained variance in yellow), the radius of the pie chart being a linear function of the total uncertainty. The bottom plots illustrate the dispersion of these proportions over the different reference regions, for each variable and season.

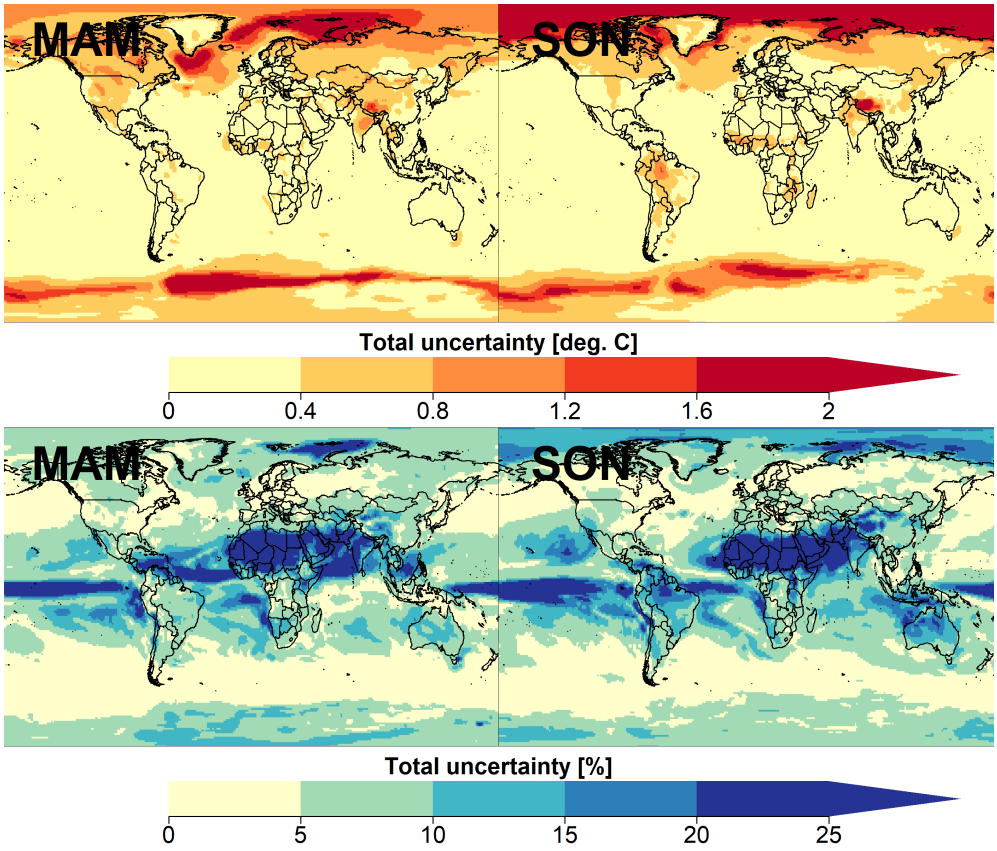

Fig. S15 Total uncertainty $TU(2)$ (square root of the total variance) at a $1^\circ \times 1^\circ$ resolution, for absolute changes of mean temperature (tas) and relative changes of total precipitation (pr) in spring (MAM) and autumn (SON) at a warming level of $+2$°C compared with the pre-industrial period (1850–1900).

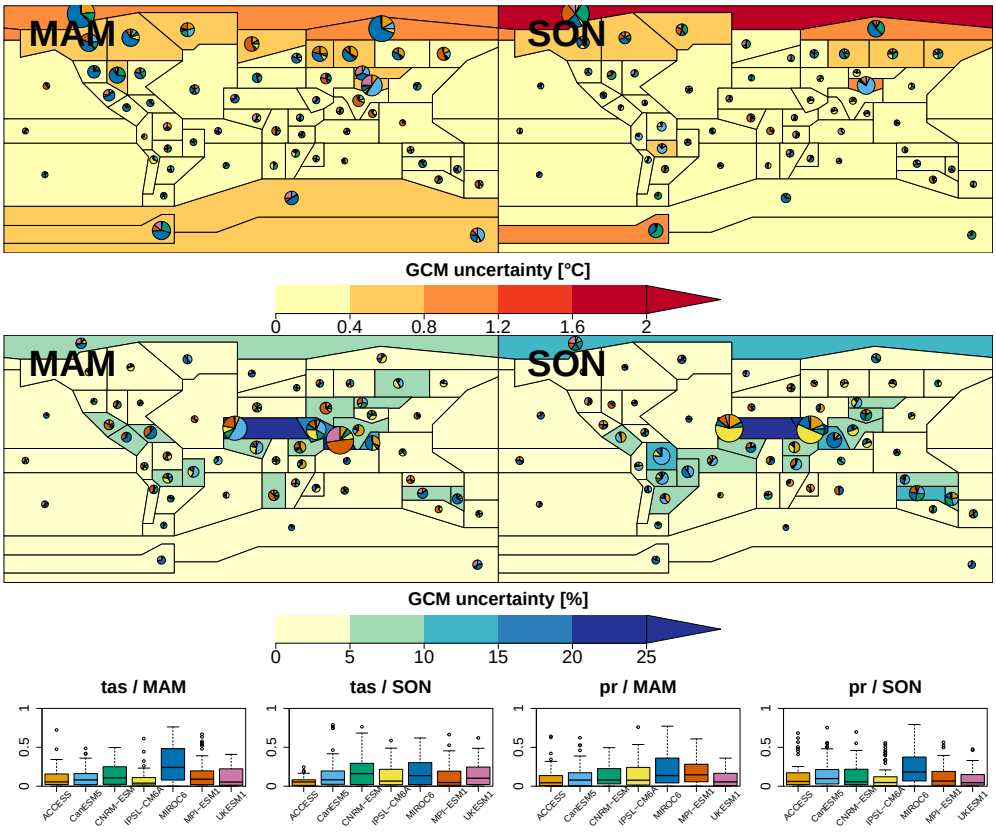

Fig. S16 GCM uncertainty (square root of the variance of the main GCM effects) for absolute changes of mean temperature (tas) and relative changes of total precipitation (pr) in spring (MAM) and autumn (SON) at a warming level of +2°C compared with the pre-industrial period (1850–1900). For each reference region, the pie chart provides the contributions of the different GCMs to the GCM uncertainty, the radius of the pie chart being a linear function of the GCM uncertainty. The bottom plots illustrate the dispersion of these proportions over the different reference regions, for each variable and season.

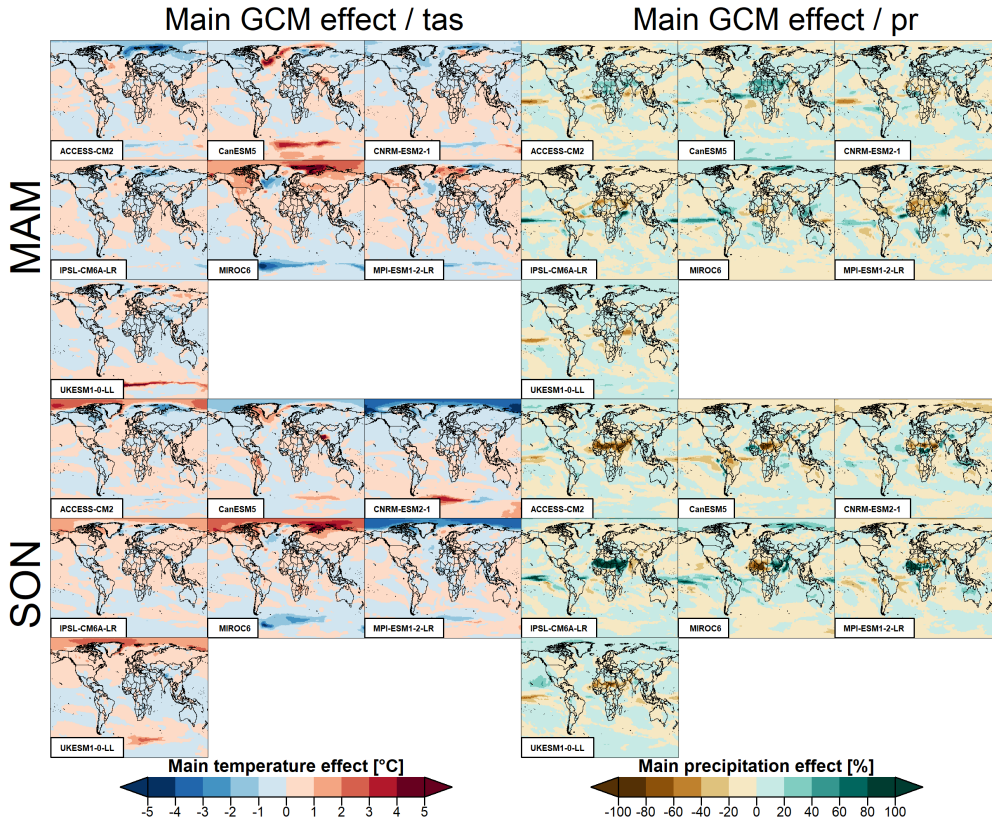

Fig. S17 Main GCM effects at a 1° × 1° resolution for absolute temperature and relative precipitation changes, in spring (MAM) and autumn (SON) at a warming level of +2°C compared with the pre-industrial period (1850–1900).

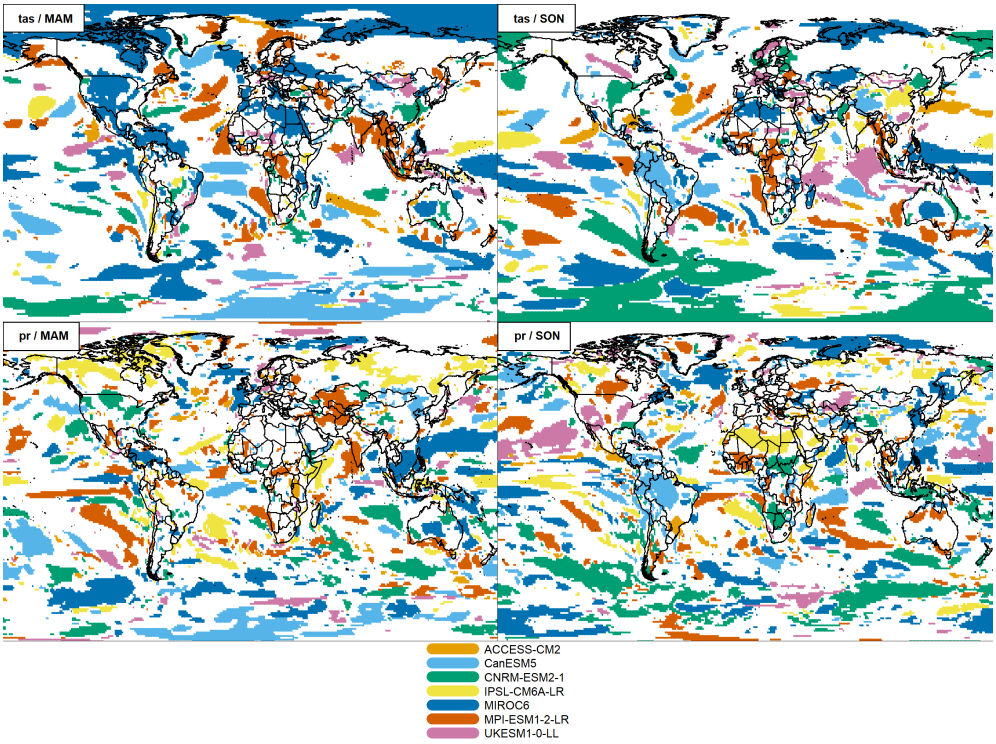

Fig. S18 GCM with a contribution greater than 50% to the GCM uncertainty at a 1° × 1° resolution for absolute temperature and relative precipitation changes, in spring (MAM) and autumn (SON) at a warming level of +2°C compared with the pre-industrial period (1850–1900).

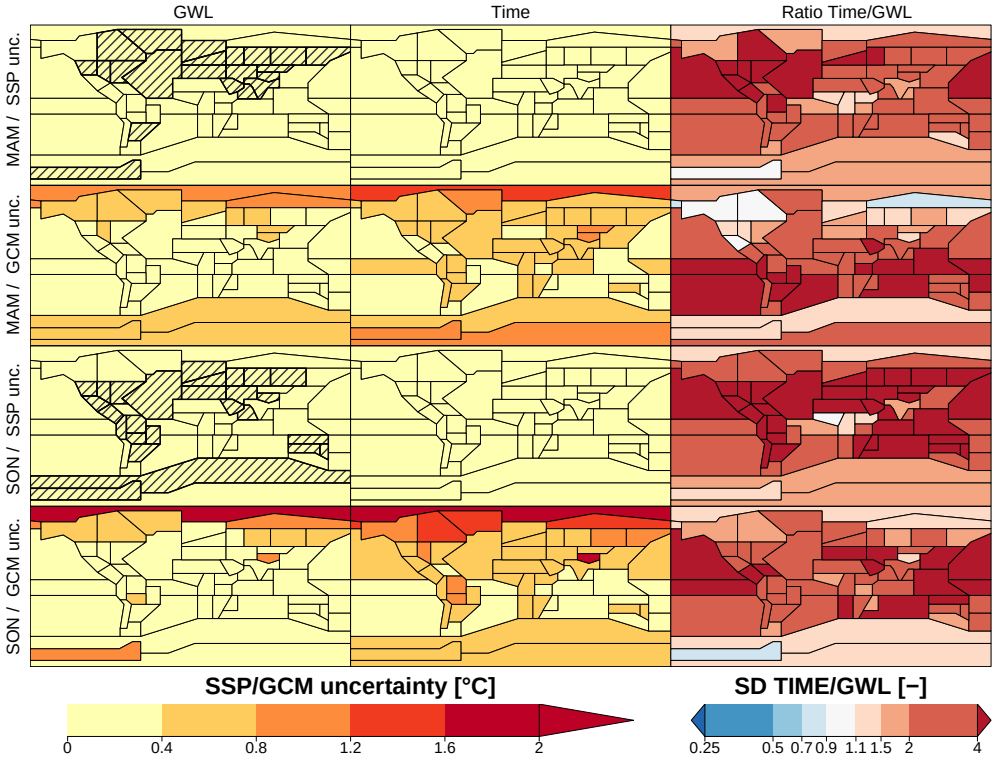

Fig. S19 Uncertainties (square root of the variances) for absolute changes of mean temperature (tas) in spring (MAM) and autumn (SON) when they are obtained for a warming level of 2°C ("GWL") or the year 2038 ("time") compared with the pre-industrial period 1850-1900. The third column shows the ratio between both uncertainties, e.g. $\sqrt{V_{GCM}(2038)}/\sqrt{V_{GCM}(2)}$ for GCM uncertainties. The first and third lines show the SSP uncertainty $\sqrt{V_{SSP}}$ and the second and fourth lines the GCM uncertainty $\sqrt{V_{GCM}}$. Hashed regions indicate non-significant variances according to the standard F-test of the ANOVA.

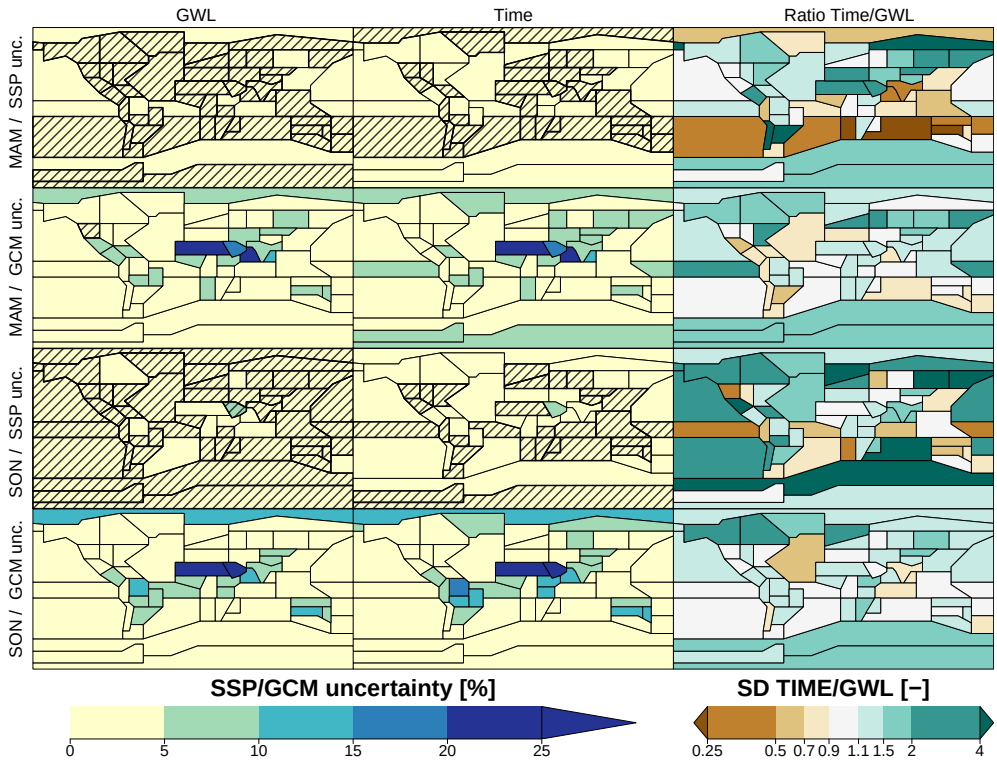

Fig. S20 Same as Figure S19 for relative changes of total precipitation (pr).